Plastic Deformation of a Perforated Sheet With Non-Uniform Circular Holes Along the Thickness Direction

Fuh-Kuo Chen
e-mail: fkchen@w3.me.ntu.edu.tw

Yi-Che Lee

Department of Mechanical Engineering,
National Taiwan University,
Taipei, Taiwan, ROC

For a perforated sheet with circular holes, used in shadow masks, the diameter of the circular hole varies through the thickness, and the non-uniform circular holes are arranged in a triangular pattern. In order to simplify the analysis, a perforated sheet with equivalent circular holes of uniform diameter is proposed such that its plastic behavior is similar to that with the given non-uniform circular holes. In this study, a yield criterion is discussed for the perforated sheet with uniform circular holes by employing an equivalent continuum approach, which is then applied to examine the plastic deformation of the perforated sheet with non-uniform circular holes. The analytical results predicted by the theory, including those for the apparent yield stresses and strain ratios, are verified by the results obtained from the finite element analysis and also from experiments.
[DOI: 10.1115/1.1526127]

1 Introduction

Perforated sheets with circular holes arranged in a triangular pattern are widely used in the metal industry. In most applications, the diameter of each circular hole is uniform in the thickness direction of the perforated sheet, such as tube sheets employed in heat-exchanger equipment [1]. However, the diameter of each hole varies through the thickness of the perforated sheet in the case of shadow masks used in high-resolution color picture tubes [2] as illustrated in Fig. 1. Such a hole is termed "non-uniform circular hole" in this paper. For the proper design and manufacture of products made of perforated sheets with non-uniform circular holes, the characterization of the plastic deformation of the perforated sheet, including the definition of a yield criterion and its associated flow rule, is fundamental.

Previous investigations of the plastic deformation of perforated sheets [3–7] focused on sheets with circular holes that are uniform in the thickness direction, and are arranged in a triangular pattern. Those investigators proposed various yield criteria for the perforated sheets with the help of an equivalent continuum approach after assuming a plane stress condition and a state of isotropy of the base metal of the perforated sheet. The yield criteria proposed by them are not applicable, however, to describe the plastic behavior of the perforated sheets with non-uniform holes.

For perforated sheets with non-uniform circular holes, the plastic state varies in the thickness direction, and a three-dimensional model is generally needed for a rigorous analysis of the deformation behavior. However, Baik et al. [8–10] proposed a simplified two-dimensional model, assuming that a perforated sheet with non-uniform circular holes behaves in the same way as that with uniform circular holes having a mean diameter. They also considered the yielding at the center of the minimum ligament width to identify the overall yield condition of the perforated sheet. However, the stress state at the center of the minimum ligament width has been found to be inadequate to describe the initial yielding of the perforated sheet.

In the present study, the perforated sheet with non-uniform circular holes arranged in a triangular array, as shown in Fig. 1, was investigated. The diameter of an auxiliary uniform circular hole, in which the plastic behavior is considered as equivalent to that for the non-uniform circular hole, was defined at the outset, the considered hole being called "equivalent uniform circular hole" in this paper. A perforated sheet with equivalent uniform circular holes was supposed to behave in a manner similar to that with non-uniform circular holes in the plastic range of deformation. A theoretical model was then developed in the present study to determine the initial yielding of the perforated sheet with uniform circular holes by examining the average values of the stress components along the entire minimum ligament width, instead of

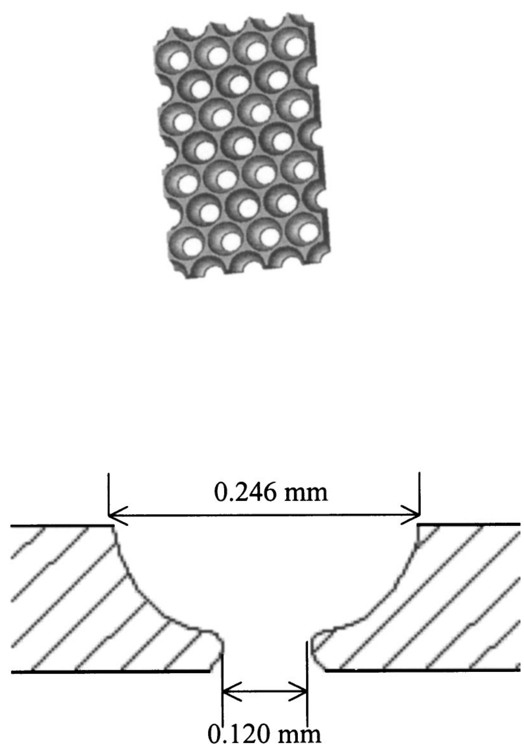

Fig. 1 Geometry of the non-uniform circular hole

Contributed by the Materials Division for publication in the JOURNAL OF ENGINEERING MATERIALS AND TECHNOLOGY. Manuscript received by the Materials Division June 9, 2001; revision received February 3, 2002. Associate Editor: H. M. Zbib.

those at the center of this ligament. An appropriate yield criterion and its associated flow rule were then developed for the plastic deformation of perforated sheets with uniform circular holes, and subsequently applied to perforated sheets with non-uniform circular holes on the basis of the proposed equivalence. The proposed theoretical models were validated by the finite element analysis and also by experimental results.

2 The Diameter of an Equivalent Uniform Circular Hole

Yielding generally occurs in the base metal along the minimum ligament width when a perforated sheet with uniform circular holes is loaded, as shown in Fig. 2. The effective stress in the base metal along the minimum ligament is equal to the yield stress of the base metal when the perforated sheet begins to yield. By assuming that the base metal of the perforated sheet is perfectly plastic, and yielding occurs instantaneously and uniformly across the thickness, the yielding load F under a uniaxial loading of a unit cell, as shown in Fig. 2, in the perforated sheet with non-uniform holes can be expressed as

$$F=\int_0^t [P_y-a(z)]\sigma_y dz, \tag{1}$$

where σ_y is the yield stress of the base metal of the perforated sheet. The diameter of the non-uniform circular hole $a(z)$ varies through the thickness of the perforated sheet, where z is the distance in the thickness direction of the perforated sheet, as shown in Fig. 3. P_y is the perforation pitch and t is the thickness of the perforated sheet, as illustrated in Fig. 2.

On the other hand, the yielding load of the perforated sheet with equivalent uniform circular holes, where the stress is uniformly distributed across the thickness of the perforated sheet, can be written as

$$F=t\times(P_y-\bar{a})\sigma_y, \tag{2}$$

where $\bar{a}$ is the diameter of the equivalent uniform circular hole, as depicted in Fig. 3(b).

The diameter $\bar{a}$ of the equivalent uniform circular hole is obtained by equating the yielding load for the perforated sheet with non-uniform circular holes with that having equivalent uniform circular holes. It follows from equations (1) and (2) that

$$\bar{a}=\frac{1}{t}\int_0^t a(z)dz. \tag{3}$$

The diameter of the equivalent circular hole evaluated by using Eq. (3) will be validated by the finite element analysis and experiments, which compare the apparent stress-strain relation of the perforated sheet with equivalent uniform circular holes with that containing non-uniform circular holes. The detailed validation is depicted in the section of results and discussions.

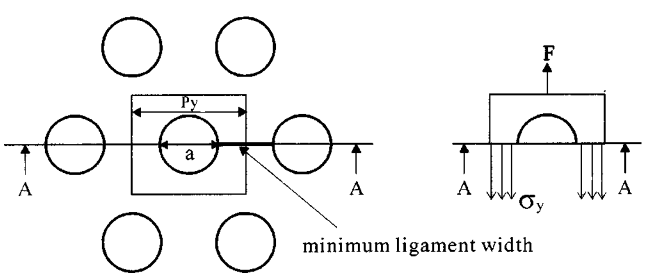

Fig. 2 Triangular pattern of circular holes showing yielding along the minimum ligament width

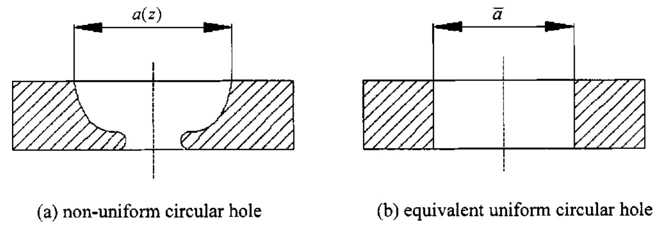

Fig. 3 Non-uniform circular hole and the equivalent uniform circular hole: (a) non-uniform circular hole; and (b) equivalent uniform circular hole

3 A Yield Criterion for the Perforated Sheet With Uniform Circular Holes

For the given geometrical configuration of the perforated sheet, the x and y directions are chosen coincidentally with the directions of the principal axes of anisotropy in the perforated sheet with uniform circular holes arranged in a uniform triangular pattern, as illustrated in Fig. 4. The ligament ratio ρ is defined as the ratio of the ligament width W to the perforation pitch P in a unit cell, as displayed by the area $ABCD$ in Fig. 4, where ρ_x and ρ_y are the ligament ratios in the x and y directions, respectively, and are given by $\rho_x=W_x/P_x$ and $\rho_y=W_y/P_y$ where W_x, P_x and W_y, P_y are ligament width and perforation pitch normal to the x and y directions, respectively. The significance of the equivalent uniform circular hole for the geometrical configuration of the perforated sheet with non-uniform circular holes for shadow masks is illustrated in Fig. 3. The ligament ratio ρ_y of the perforated sheet with equivalent uniform circular holes generally lies within a limited range of low values of the ligament ratio, and is approximately 0.23 for most shadow masks. Therefore, a yield criterion was developed to investigate the plastic deformation of the perforated sheet with uniform circular holes for sufficiently low ligament ratios. Earlier works [7–10] assumed yielding to begin along the ligaments defined by the lines AB and AO shown in Fig. 4. However, the stress distribution of the perforated sheet furnished by the finite element simulations, performed in the present study, indicates yielding to occur in the ligament along AO when the ligament ratio ρ_y is less than 0.5. By considering yielding only in the ligament along AO, a theoretical model that defines a yield criterion for the perforated sheet was developed in this paper.

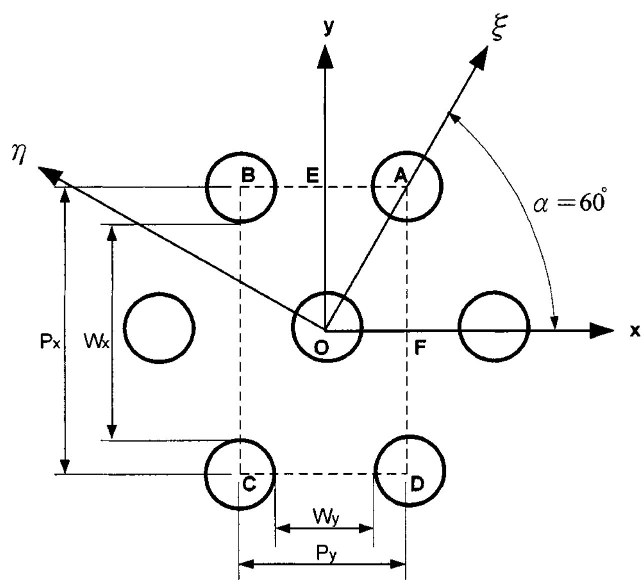

Fig. 4 Circular holes arranged in a triangular pattern

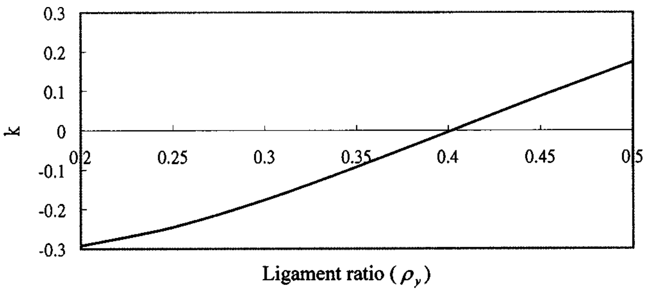

Fig. 5 Values of *k* for various ligament ratios

3.1 Yield Criterion. Consider an equivalent sheet metal that has the same overall dimensions and mechanical properties as those of the perforated sheet metal. The stresses existing in the equivalent sheet metal are only apparent stresses, defined as the external forces divided by the equivalent areas upon which the forces act. Let S_x and S_y be the apparent stresses acting in the unit cell ABCD, as shown in Fig. 4, in the x and y directions, respectively, which are presumed to be uniform in the equivalent continuum model. The (x,y) components of the apparent stress can be transformed into those referred to the (ξ,η) coordinates under biaxial loading in the x and y directions as indicated in Fig. 4. It is easily shown that

$$S_\xi=\frac{1}{4}(S_x+3S_y),$$
$$S_\eta=\frac{1}{4}(3S_x+S_y), \tag{4}$$
$$S_{\xi\eta}=-\frac{\sqrt{3}}{4}(S_x-S_y).$$

Dividing the apparent stresses by the corresponding ligament ratios, the mean values of the true stresses across the ligament in the base metal are obtained as

$$\overline{\sigma}_\eta=\frac{S_\eta\times P_\eta}{W_\eta}=\frac{S_\eta\times P_y}{W_y}=\frac{S_\eta}{\rho_\eta}=\frac{1}{4\rho_y}(3S_x+S_y), \tag{5}$$

$$\overline{\sigma}_{\xi\eta}=\frac{S_{\xi\eta}\times P_\eta}{W_\eta}=\frac{S_{\xi\eta}\times P_y}{W_y}=\frac{S_{\xi\eta}}{\rho_\eta}=-\frac{\sqrt{3}}{4\rho_y}(S_x-S_y), \tag{6}$$

where $\overline{\sigma}_\eta$ and $\overline{\sigma}_{\xi\eta}$ are the mean true normal and shear stresses across the ligament in the η direction. It should be noted that according to the geometry of the perforation, $W_\eta=W_y$, $P_\eta=P_y$, and $\rho_\eta=\rho_y$.

In order to obtain the mean true normal stress along the ligament in the ξ direction, it does not seem to be realistic to define it as the ratio of the apparent stress, S_ξ, to the corresponding ligament ratio, ρ_ξ. In this study, a factor of k is introduced to modify the definition of the mean true normal stress in the ξ direction, which may be expressed as

$$\overline{\sigma}_\xi=\frac{k\times S_\xi}{\rho_\xi}=\frac{k}{\rho_x}\times\frac{1}{4}(S_x+3S_y) \tag{7}$$

where $\rho_\xi=\rho_x$ according to the geometry of the perforation pattern, displayed in Fig. 4. In the present study, a theoretical model, using the method of complex stress potentials based on the theory of elasticity, developed by Isida and Igawa [11], was adopted to calculate the distribution of the transverse normal stress σ_ξ along the minimum ligament width AO. The value of k, which is a function of the ligament ratio [12], was then determined according to Eq. (7), and was plotted in Fig. 5 for $\rho_y\leqslant 0.5$.

As mentioned earlier, this study assumes the base metal of the perforated sheet to be isotropic and the plastic deformation of the perforated sheet to occur under plane stress condition. Under the plane-stress condition, the von Mises yield criterion applied to the base metal of the perforated sheet furnishes

$$\overline{\sigma}_\xi^2-\overline{\sigma}_\xi\overline{\sigma}_\eta+\overline{\sigma}_\eta^2+3\overline{\sigma}_{\xi\eta}^2=Y_b^2, \tag{8}$$

where Y_b is the uniaxial yield stress of the base metal of the perforated sheet. The yield criterion for the perforated sheet is obtained by substituting the stresses in (5), (6), and (7) into the von Mises yield criterion (8). The result is

$$\left(\frac{1}{16}\right)\left[\left(\frac{k^2}{\rho_x^2}-\frac{3k}{\rho_x\rho_y}+\frac{18}{\rho_y^2}\right)S_x^2+\left(\frac{6k^2}{\rho_x^2}-\frac{10k}{\rho_x\rho_y}-\frac{12}{\rho_y^2}\right)S_xS_y+\left(\frac{9k^2}{\rho_x^2}-\frac{3k}{\rho_x\rho_y}+\frac{10}{\rho_y^2}\right)S_y^2\right]=Y_b^2. \tag{9}$$

The yield criterion expressed by (9) is not general, however, for the plastic behavior under arbitrary stress states. We therefore add a shear term, S_{xy}, into the yield criterion (9), to obtain the modified form

$$\left(\frac{1}{16}\right)\left[\left(\frac{k^2}{\rho_x^2}-\frac{3k}{\rho_x\rho_y}+\frac{18}{\rho_y^2}\right)S_x^2+\left(\frac{6k^2}{\rho_x^2}-\frac{10k}{\rho_x\rho_y}-\frac{12}{\rho_y^2}\right)S_xS_y+\left(\frac{9k^2}{\rho_x^2}-\frac{3k}{\rho_x\rho_y}+\frac{10}{\rho_y^2}\right)S_y^2\right]+N\times S_{xy}^2=Y_b^2 \tag{10}$$

where N is the anisotropic coefficient of the shear term, which is yet to be determined.

For perforated sheets with uniform circular holes arranged in a triangular pattern, there are three axes of symmetry for the associated state of anisotropy. Since the degree of anisotropy is small [7], the anisotropic behavior of the perforated sheet can be approximately described by assuming a state of planar isotropy. Then the yield stress in pure shear with respect to the anisotropic axes should be the same as that in simple shear with respect to the same axes. A state of pure shear is given by

$$S_x=\tau,\quad S_y=-\tau\quad\text{and}\quad S_{xy}=0, \tag{11}$$

where τ is the associated yield shear stress. Substituting Eq. (11) into Eq. (10), we obtain

$$\frac{\tau^2}{16}\left(\frac{4k^2}{\rho_x^2}+\frac{4k}{\rho_x\rho_y}+\frac{40}{\rho_y^2}\right)=Y_b^2. \tag{12}$$

In the case of simple shear represented by

$$S_x=S_y=0,\quad\text{and}\quad S_{xy}=\tau, \tag{13}$$

we have

$$N\times\tau^2=Y_b^2. \tag{14}$$

Considering the equality of τ given by (12) and (14), we obtain the coefficient N of the shear term as

$$N=\frac{1}{16}\left(\frac{4k^2}{\rho_x^2}+\frac{4k}{\rho_x\rho_y}+\frac{40}{\rho_y^2}\right). \tag{15}$$

The yield criterion is now determined completely, and is rewritten as

$$\left(\frac{1}{16}\right)\left[\left(\frac{k^2}{\rho_x^2}-\frac{3k}{\rho_x\rho_y}+\frac{18}{\rho_y^2}\right)S_x^2+\left(\frac{6k^2}{\rho_x^2}-\frac{10k}{\rho_x\rho_y}-\frac{12}{\rho_y^2}\right)S_xS_y+\left(\frac{9k^2}{\rho_x^2}-\frac{3k}{\rho_x\rho_y}+\frac{10}{\rho_y^2}\right)S_y^2+\left(\frac{4k^2}{\rho_x^2}+\frac{4k}{\rho_x\rho_y}+\frac{40}{\rho_y^2}\right)S_{xy}^2\right]=Y_b^2. \tag{16}$$

If the uniform circular hole diameter is zero, $\rho_x=\rho_y=1$, and the apparent stresses of the perforated sheet are the same as the mean true stresses in the base metal, where k is also equal to unity, the yield criterion (16) reduces to the von Mises yield criterion.

The apparent yield stresses for the perforated sheet can be predicted by using the yield criterion. Assuming a uniaxial tension in the y direction, the apparent yield stress Y_y can be expressed as

$$Y_y = 4 \times \left(\frac{9k^2}{\rho_x^2} - \frac{3k}{\rho_x \rho_y} + \frac{10}{\rho_y^2} \right)^{-1/2} Y_b. \tag{17}$$

Similarly, the apparent yield stress in the x direction, Y_x, can be determined from

$$Y_x = 4 \times \left(\frac{k^2}{\rho_x^2} - \frac{3k}{\rho_x \rho_y} + \frac{18}{\rho_y^2} \right)^{-1/2} Y_b. \tag{18}$$

Considering a uniaxial tension in the direction inclined at an angle of 45° to the x direction, the apparent yield stress Y_{45} is obtained as

$$Y_{45} = 8 \times \left(\frac{20k^2}{\rho_x^2} - \frac{12k}{\rho_x \rho_y} + \frac{56}{\rho_y^2} \right)^{-1/2} Y_b. \tag{19}$$

3.2 Associated Flow Rule. The associated flow rule can be established by assuming that the yield function $f(S_{ij})$ is identical to the plastic potential. The components of the apparent strain rate $\dot{e}_{ij}$ are therefore defined as

$$\dot{e}_{ij} = \dot{\lambda} \frac{\partial f}{\partial S_{ij}}, \tag{20}$$

where $\dot{\lambda}$ is a factor of proportionality. Since the apparent strain e_{ij} may be substituted for the apparent strain rate as the stress ratios do not vary significantly over a small range of strains [13], Eq. (20) becomes

$$e_{ij} = \lambda \frac{\partial f}{\partial S_{ij}}. \tag{21}$$

where λ is a positive scalar quantity.

Using the yield function of (16) substituted into the associated flow rule (21), we obtained the normal strains as

$$e_x = \lambda \left(\frac{1}{4} \right)^2 \left[2 \left(\frac{k^2}{\rho_x^2} - \frac{3k}{\rho_x \rho_y} + \frac{18}{\rho_y^2} \right) S_x + \left(\frac{6k^2}{\rho_x^2} - \frac{10k}{\rho_x \rho_y} - \frac{12}{\rho_y^2} \right) S_y \right], \tag{22}$$

$$e_y = \lambda \left(\frac{1}{4} \right)^2 \left[\left(\frac{6k^2}{\rho_x^2} - \frac{10k}{\rho_x \rho_y} - \frac{12}{\rho_y^2} \right) S_x + 2 \left(\frac{9k^2}{\rho_x^2} - \frac{3k}{\rho_x \rho_y} + \frac{10}{\rho_y^2} \right) S_y \right]. \tag{23}$$

For a uniaxial tension in the y direction, the apparent strain ratio R_y defined as the ratio of the negative apparent strain e_x in the x direction to the apparent strain e_y in the y direction, can be expressed as

$$R_y = -\frac{e_x}{e_y} = -\frac{\left(\frac{6k^2}{\rho_x^2} - \frac{10k}{\rho_x \rho_y} - \frac{12}{\rho_y^2} \right)}{2 \left(\frac{9k^2}{\rho_x^2} - \frac{3k}{\rho_x \rho_y} + \frac{10}{\rho_y^2} \right)}. \tag{24}$$

Similarly, for a uniaxial tension in the x direction, the apparent strain ratio R_x is found to be

$$R_x = -\frac{e_y}{e_x} = -\frac{\left(\frac{6k^2}{\rho_x^2} - \frac{10k}{\rho_x \rho_y} - \frac{12}{\rho_y^2} \right)}{2 \left(\frac{k^2}{\rho_x^2} - \frac{3k}{\rho_x \rho_y} + \frac{18}{\rho_y^2} \right)}. \tag{25}$$

4 Finite Element Analysis

The finite element simulations were performed to analyze and validate the analysis of the local deformation of the perforated sheet subjected to uniaxial and biaxial tension. In view of the symmetry in the geometric configuration of the perforated sheet, a repetitive portion, as depicted by the area OFAE in Fig. 4, is adopted as a unit cell for the finite element simulations. For the deformation simulation of the unit cell OFAE, the symmetry edges FO and OE have to be fixed in the direction of symmetry. Under a uniaxial tension in the x direction, the side FA is given a constant displacement and the deformation of the side EA is also assumed uniform. Under a uniaxial tension in the y direction, the side AE is given a constant displacement and the deformation of the side FA is also assumed uniform. The simulation results, including the apparent stress-strain curve, apparent yield stresses, and apparent strain ratios, are compared with those predicted by both the theoretical analysis and experiments.

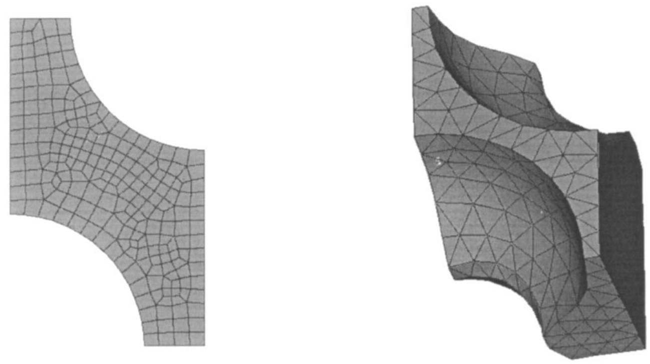

(*a*) (*b*)

Fig. 6 Finite element models for a unit cell: (*a*) two-dimensional; and (*b*) three-dimensional

The finite element simulations were first conducted for the perforated sheet with non-uniform circular holes, used in shadow masks illustrated in Fig. 6(*b*), in order to verify the theoretical prediction of the equivalent uniform circular hole diameter, as well as the apparent stress-strain relation for the perforated sheet. The diameter of the non-uniform circular hole varies from 0.246 mm to 0.120 mm in the thickness direction of the perforated sheet, as illustrated in Fig. 1. The apparent stress-strain relation for the perforated sheets with uniform circular holes, within a limited range, are also simulated by the finite element model, shown in Fig. 6(*a*). The predicted diameter of the equivalent uniform circular holes for the shadow masks is approximately 0.20 mm, while the uniform circular holes of diameters, 0.18 mm, 0.20 mm and 0.22 mm are adopted to obtain the prediction values. The theoretical model is justified by comparing the apparent stress-strain relation for the perforated sheet with uniform and non-uniform circular holes. The finite element software ABAQUS was employed in the present study, and the plane stress element was used to perform simulations.

5 Experimental Work

Invar (Fe-36Ni) and stainless steel (AISI-304) were used as the base materials to manufacture various perforated sheets. Young's modulus and Poisson's ratio for invar are 151 GPa and 0.28, respectively, and the corresponding flow curve is approximately represented by the empirical equation $\bar{\sigma} = 229.9 + 1280\bar{\varepsilon}$ (MPa). Young's modulus and Poisson's ratio for stainless steel are 198 GPa and 0.30, respectively, and its flow curve is approximately given by $\bar{\sigma} = 308 + 1449\bar{\varepsilon}$ (MPa). The significance of the adoption of an equivalent uniform circular hole could be established by comparing the experimental results for the apparent yield stress ratios and the apparent strain ratios with those predicted by the proposed yield criterion under the assumption of a plane-stress condition.

The 0.137 mm thick perforated sheet with non-uniform circular holes made of invar was investigated to verify the equivalent uniform circular hole for the given non-uniform hole used in shadow masks. The invar sheet metal was etched to make the perforation with various uniform circular holes with a given perforation pitch, and tensile tests were performed in order to confirm the equivalent uniform circular hole model. The selected hole diameters were 0.18 mm, 0.20 mm and 0.22 mm, and a perforation pitch of 0.26 mm was adopted for the purpose.

The experimental results for the uniaxial tensile tests, furnishing the apparent yield stress ratios and apparent strain ratios, were used not only to verify the theoretical results but also to confirm the results determined by the finite-element method. Perforated sheets with ligament ratios $\rho_y = 0.25$, 0.3, 0.4 and 0.5 were prepared for the experimental work. The sheets were cut from a 1.2 mm thick stainless steel sheet along both the x and y directions to prepare the tensile specimens. The distance between the centers of two adjacent holes was subsequently recorded to determine the material flow during the deformation. The average distance between the centers of two adjacent holes in the loading and the transverse directions was measured after the test, and then compared with that before the test to evaluate the apparent strain ratios.

6 Results and Discussions

The maximum and minimum diameters of the non-uniform holes in a 0.137 mm thick shadow mask are 0.246 mm and 0.120 mm, respectively, as depicted in Fig. 1, while the diameter of the predicted equivalent uniform circular hole is found to be 0.20 mm approximately. The relation between the apparent stress and apparent strain obtained from the finite element analysis and experiments, for perforated sheets with the non-uniform circular holes, and also those with various diameters of uniform circular holes, are shown in Figs. 7 and 8, respectively. It can be seen from both the figures that the variation of the apparent stress with apparent strain for the perforated sheet with non-uniform circular holes is very close to that for the perforated sheet with uniform circular holes having a diameter of 0.20 mm. This observation agrees very well with that predicted by the theoretical model.

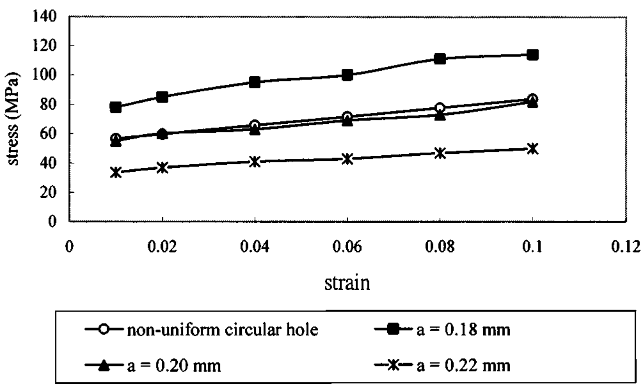

Fig. 7 Apparent stress and strain relation obtained from FEM for uniaxial tension in the *y* direction

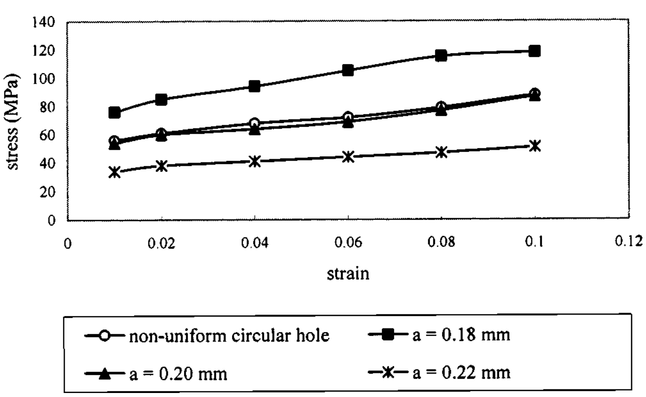

Fig. 8 Apparent stress and strain relation obtained from experiments for uniaxial tension in the *y* direction

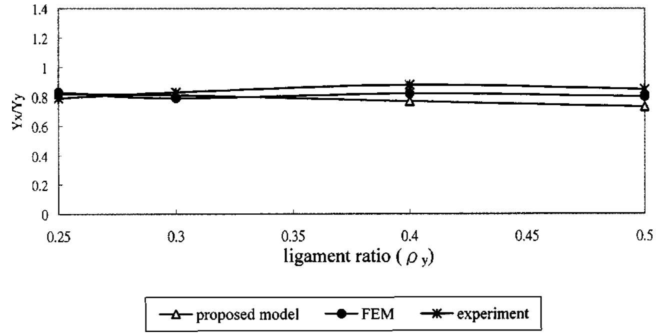

Fig. 9 Comparison of apparent yield stress ratios (Y_x/Y_y)

The stress distributions along the ligaments AO and AB, shown in Fig. 4, were analyzed by the finite element method for the perforated sheet with ligament ratios of $\rho_y = 0.154$, 0.285, 0.462, 0.515, and 0.615, respectively, to confirm the deformation model for low ligament ratios. The true effective stress distributions along the minimum ligaments obtained by the finite element analysis reveal that the location of the maximum true effective stress is very nearly in the minimum ligament when the ligament ratio is small. This result lends support to the assumption that the initial yielding occurs in the minimum ligament.

The effectiveness of the proposed yield criterion for the perforated sheet with uniform circular holes and low ligament ratios is established by comparing the predicted values of the apparent yield stress ratios, Y_x/Y_y and Y_{45}/Y_b, and the apparent strain ratios, R_x and R_y, with those obtained from the finite element

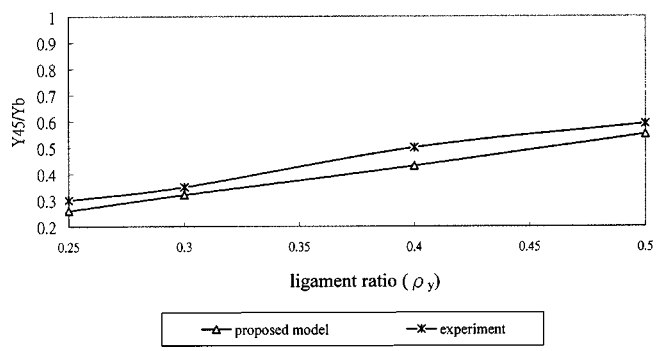

Fig. 10 Comparison of apparent yield stress ratios (Y_{45}/Y_b)

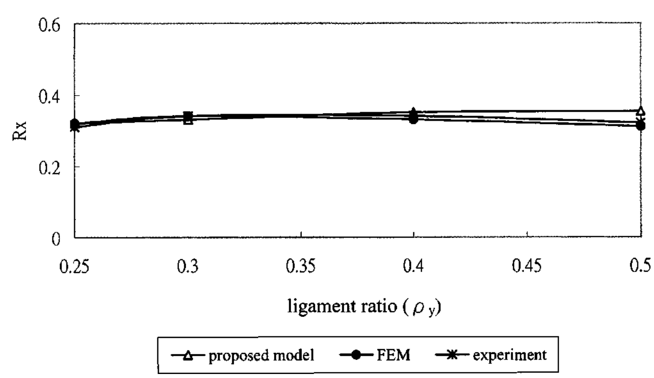

Fig. 11 Comparison of the apparent strain ratios R_x

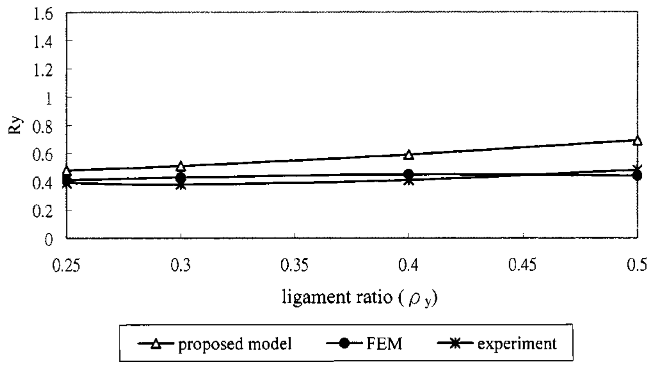

Fig. 12 Comparison of the apparent strain ratios R_y

analysis, as well as with the experimental results. A graphical comparison of the apparent yield stress ratios, Y_x/Y_y is made in Fig. 9, which indicates that the predicted values agree with those obtained from the finite element analysis and from experiments. Over a range of relatively large ligament ratios, the theoretical model predicts slightly lower apparent yield stress ratios, though the difference is not significant. The apparent yield stress ratios, Y_{45}/Y_b, predicted by the proposed yield criterion and derived from the experimental tests are shown in Fig. 10. The agreement is seen to be satisfactory, although a slightly larger difference is noted. The discrepancy is apparently due to the assumption of planar isotropy used in the derivation of the coefficient of the shear term in the yield criterion.

Figures 11 and 12 present the results for the apparent strain ratios, R_x and R_y, respectively, obtained by the theoretical analysis, the finite element simulations, and the experimental data, for various ligament ratios. It is seen in Fig. 11 that the results agree with one another both in trend and in magnitude for R_x. However, the discrepancy between the values of R_y obtained from the three methods is significantly higher when the ligament ratio is larger than 0.4, as seen in Fig. 12. This indicates the need for future research to improve the theoretical model to accomplish a better description of the plastic behavior of perforated sheets with ligament ratio greater than 0.4.

7 Conclusions

This study introduced the concept of equivalent uniform circular holes to analyze the plastic deformation of perforated sheets with non-uniform circular holes used in shadow masks. The stress-strain relation for perforated sheets containing non-uniform circular holes, obtained by the finite element method and experiments, was compared with that predicted by the proposed theoretical model to demonstrate the effectiveness of the present theory.

A new yield criterion and its associated flow rule were also developed for the analysis of the plastic deformation of perforated sheets with equivalent uniform circular holes. The assumption for the location of plastic yielding for the perforated sheet is generally not applicable over the whole range of the ligament ratio. However, the yielding of the perforated sheet with uniform circular holes, and with ligament ratios smaller than 0.5, is found to occur along the ligament width AO shown in Fig. 4. The mean values of the stress components in the base metal along the ligament width AO were therefore considered in this paper to examine the yielding of the perforated sheet. The validity of the proposed yield criterion was confirmed by comparing the predicted apparent yield stress ratios and apparent strain ratios with those obtained by the finite element analysis and experiments. The agreement was found to be good for low ligament ratios.

Acknowledgments

The authors would like to thank the National Science Council of the Republic of China for financially supporting this research under Contract No. NSC 89-2212-E-002-005. They are also grateful to Prof. J. Chakrabarty for his comments and helpful discussions.

References

[1] Gardner, K. A., 1948, ''Heat Exchanger Tube Sheet Design,'' ASME J. Appl. Mech., **70**, pp. 377–385.
[2] Doerschuk, E. E., Moscony, J. J., and Weber, D. M., 1948, ''Shadow-Mask Etching for Data-Display Tubes,'' RCA Eng., **29(2)**, pp. 67–73.
[3] O'Donnell, W. J., and Langer, B. F., 1962, ''Design of Perforated Plates,'' ASME J. Eng. Ind., **84**, pp. 307–320.
[4] Horvey, G., 1952, ''The Plane-Stress Problem of Perforated Sheet,'' ASME J. Appl. Mech., **74**, pp. 355–360.
[5] O'Donnell, W. J., and Porowski, J., 1973, ''Yield Surface for Perforated Materials,'' ASME J. Appl. Mech., **37**, pp. 260–268.
[6] Sawczuk, A., O'Donnell, W., and Porowski, J., 1975, ''Plastic Analysis of Perforated Plates for Orthotropic Yield Criteria,'' Int. J. Mech. Sci., **17**, pp. 411–421.
[7] Chen, F. K., 1993, ''Analysis of Plastic Deformation for Sheet Metals With Circular Perforations,'' J. Mater. Process. Technol., **37**, pp. 175–188.
[8] Baik, S. C., Oh, K. H., and Lee, D. N., 1995, ''Forming Limit Diagram of Perforated Sheet,'' Scr. Metall. Mater., **33**, pp. 1201–1207.
[9] Baik, S. C., Oh, K. H., and Lee, D. N., 1996, ''Analysis of the Deformation of a Perforated Sheet Under Uniaxial Tension,'' J. Mater. Process. Technol., **58**, pp. 139–144.
[10] Baik, S. C., Han, H. N., Lee, S. H., Oh, K. H., and Lee, D. N., 1997, ''Plastic Behavior of Perforated Sheets Under Biaxial Stress State,'' Int. J. Mech. Sci., **39**, pp. 781–793.
[11] Isida, M., and Igawa, H., 1991, ''Analysis of a Zig-Zag Array of Circular Holes in an Infinite Solid Under Uniaxial Tension,'' Int. J. Solids Struct., **27**, pp. 849–864.
[12] Lee, Y. C., and Chen, F. K., 2000, ''Yield Criterion for a Perforated Sheet With a Uniform Triangular Pattern of Round Holes and a Low Ligament Ratio,'' J. Mater. Process. Technol., **103**, pp. 353–361.
[13] Nadai, A., 1950, *Theory of Flow and Fracture of Solids*, McGraw-Hill.